Transferred Nuclear Overhauser Enhancement Experiments Show That the Monoclonal Antibody Strep 9 Selects a Local Minimum Conformation of a *Streptococcus* Group A Trisaccharide−Hapten†

Thomas Weimar,‡,§ Shannon L. Harris,‡ J. Bruce Pitner,|| Klaus Bock,⊥ and B. Mario Pinto*,‡

Department of Chemistry, Simon Fraser University, Burnaby, British Columbia V5A 1S6, Canada, Becton Dickinson Research Center, Research Triangle Park, North Carolina 27709-2016, and Department of Chemistry, Carlsberg Laboratory, Gamle Carlsberg Vej 10, Valby, DK-2500, Denmark

Received June 16, 1995; Revised Manuscript Received August 7, 1995⊗

ABSTRACT: Transferred nuclear Overhauser enhancement (TRNOE) experiments have been performed to investigate the bound conformation of the trisaccharide repeating unit of the *Streptococcus* Group A cell-wall polysaccharide. Thus, the conformations of propyl 3-*O*-(2-acetamido-2-deoxy-β-D-glucopyranosyl)-2-*O*-(α-L-rhamnopyranosyl)-α-L-rhamnopyranoside [C(A′)B] (**1**) as a free ligand and when complexed to the monoclonal antibody Strep 9 were examined. Improved insights about the conformational preferences of the glycosidic linkages of the trisaccharide ligand showed that the free ligand populates various conformations in aqueous solution, thus displaying relatively flexible behavior. The NOE HNAc−H2A′, which was not detected in previous work, accounts for a conformation at the β-(1→3) linkage with a ϕ angle of ~180°. Observed TRNOEs for the complex are weak, and their analysis was further complicated by spin diffusion. With the use of transferred rotating-frame Overhauser enhancement (TRROE) experiments, the amount of spin diffusion was assessed experimentally, proving that all of the observed *long-range* TRNOEs arose through spin diffusion. Four interglycosidic distances, derived from the remaining TRNOEs and TRROEs, together with repulsive constraints, derived from the absence of TRROE effects, were used as input parameters in simulated annealing and molecular mechanics calculations to determine the bound conformation of the trisaccharide. Complexation by the antibody results in the selection of one defined conformation of the carbohydrate hapten. This bound conformation, which is a local energy minimum on the energy maps calculated for the trisaccharide ligand, shows only a change from a +*gauche* to a −*gauche* orientation at the ψ angle of the α-(1→2) linkage when compared to the global minimum conformation. The results infer that the bound conformation of the *Streptococcus* Group A cell-wall polysaccharide is different from its previously proposed solution structure (Kreis et al., 1995).

Streptococcus pyogenes (Group A) is one of the primary infective agents in humans, causing streptococcal pharyngitis, some forms of pneumonia, and toxic shock-like syndrome (Read & Zabriskie, 1980; Williams, 1993). The relationship between an initial streptococcal infection and the pathogenesis of its sequelae (rheumatic fever, heart-valvular disease, glomerulonephritis, and other rheumatic disorders) is far from clear, but evidence to date suggests that cases of rheumatic fever occur only after an immunologically significant streptococcal infection (Bisno, 1985; Rotta, 1987). Patients with *Streptococcus*-related rheumatic diseases show autoimmune antibody responses, in that cross-reactivity is found between surface antigens of the bacterium and antigens of cardiac and muscle tissue (Read & Zabriskie, 1980). Cross-reactivity with heart tissue has been demonstrated both with antibodies against the M protein (Fischetti, 1989) and against the *Streptococcus* Group A cell-wall polysaccharide (Goldstein et al., 1967 & 1968).

The repeating unit of the *Streptococcus* Group A cell-wall polysaccharide consists of a poly-α-L-rhamnopyranosyl backbone composed of alternating (1→2) and (1→3) linkages to which β-D-GlcNAc[1] residues are attached at the 3-position of every second rhamnose residue (Coligan et al., 1987; Huang et al., 1986). In an ongoing project to investigate the structural and dynamic behavior of the free and antibody-bound polysaccharide, we have synthesized different oligosaccharide portions of the bacterial cell-wall polysaccharide (Pinto, 1993; Marino-Albernas et al., 1993). The conformational analysis of the free oligosaccharides has shown that these segments share common conformational and dynamic features (Kreis et al., 1995; Stuike-Prill & Pinto, 1995). The next step in the analysis is to compare

† We are grateful to the Natural Sciences and Engineering Research Council of Canada for a grant for research abroad (to B.M.P. and K.B.) and to the Heart and Stroke Foundation of British Columbia and Yukon and the Becton Dickinson Research Center for financial support. We are also grateful to the Deutsche Forschungsgemeinschaft (DFG) for a research fellowship [to T.W. (WE 1818/1-1)].

* Author to whom correspondence should be addressed.

‡ Simon Fraser University.

§ Present address: Institute for Chemistry, Medical University Luebeck, Ratzeburger Allee 160, D-23538, Luebeck, Germany.

|| Becton Dickinson Research Center.

⊥ Carlsberg Laboratory.

⊗ Abstract published in *Advance ACS Abstracts,* September 15, 1995.

[1] Abbreviations: HOHAHA, homonuclear Hartmann−Hahn; NOE, nuclear Overhauser enhancement; NOESY, nuclear Overhauser and exchange spectroscopy; ROE, rotating-frame Overhauser enhancement; ROESY, rotating-frame Overhauser spectroscopy; TRNOE and TRROE, transferred nuclear and rotating-frame Overhauser enhancement, respectively; 1D and 2D, one- and two-dimensional; gg, *gauche gauche*; PBS, phosphate-buffered saline; D_2O, deuterium oxide; Rha, α-L-rhamnopyranose; GlcNAc, *N*-acetyl-D-glucosamine; BSA, bovine serum albumin.

0006-2960/95/0434-13672$09.00/0

these features to those of the oligosaccharides when bound by specific antibodies. This protocol should lead to a greater appreciation of the requirements of immunodiagnostic reagents and the autoimmune response with human heart and muscle tissue antigens.

TRNOE (Balaram et al., 1972a,b; Albrandt et al., 1979; Clore & Gronenborn, 1982, 1983) experiments have proven to be a powerful tool in the investigation of protein-bound conformations of ligand molecules in exchange [for recent reviews see Ni and Scheraga (1994), Lian et al. (1994), and Campbell and Sykes (1993)]. A major concern in interpreting TRNOE data is the question of whether the observed effects arise from direct cross-relaxation or spin diffusion. In the fast exchange regime where TRNOEs are observable, the average ligand molecule spends only a fraction of the actual experimental mixing time in the bound state where it is exposed to spin diffusion. On the other hand, the receptor proteins are often rather large, and spin diffusion in the bound state can therefore be very effective. Theoretical calculations (Ni & Scheraga, 1994; Lian et al., 1994; Campbell & Sykes, 1991) have shown that spin diffusion gets stronger when the ligand to receptor ratio is high and when the related distances are rather long. Thus, the use of very short experimental mixing times (30 ms) (Lian et al., 1994) or low ligand concentrations (Campbell & Sykes, 1991) were suggested to circumvent spin diffusion. A rigorous theoretical treatment of the TRNOEs (Ni & Zhu, 1994; Ni & Scheraga, 1994; Lian et al., 1994) based on the complete relaxation matrix approach (Boelens et al., 1989; Borgias & James, 1989) takes spin diffusion into account but was also not always possible, because of the lack of knowledge of the protein structure and the dissociation rate constant (off rate) for the complex under investigation. There are, however, new methods for determining off rates (Davis et al., 1994) and that account for spin diffusion which do not rely on a knowledge of protein structure (Lai et al., 1993; Constantine et al., 1995). In all these cases, NMR spectroscopy offers another way to address the amount of observed spin diffusion with the ROESY experiment (Bothner-By et al., 1994; Bax & Davis, 1985) in which spin diffusion effects show the opposite sign to effects arising from direct cross-relaxation. To the best of our knowledge, there are four reports in which the question of spin diffusion in TRNOE spectra has been addressed with ROESY experiments (Lian et al., 1994; Perlman et al., 1994; Arepalli et al., 1995; Asensio et al., 1995).

To date, two TRNOE investigations of antibody/carbohydrate systems have been described in the literature. During the writing of this paper, Glaudemans and co-workers (Glaudemans et al., 1990; Arepalli et al., 1995) reported a revision of their first report on the antibody-bound conformation of a flexible, 1→6-linked disaccharide ligand, because the TRNOE effect on which the structure determination had been based resulted from a protein-mediated spin diffusion effect. The system on which most information is available is the anti-*Salmonella* antibody Se155-4. This antibody was studied with various ligands using calorimetry (Sigurskjold et al., 1991; Sigurskjold & Bundle, 1992; Bundle et al., 1994a), X-ray crystallography (Cygler et al., 1991; Bundle et al., 1994b), and NMR experiments (Bundle et al., 1994b). It was shown that only a trisaccharide portion of larger oligosaccharides is bound by the antibody, with one of the monosaccharide residues deeply buried in the antibody binding site. The experimental TRNOE data showed that the sum of two different conformations of the trisaccharide are in accord with the observed TRNOEs; one of these conformations was identical to the bound conformation determined by X-ray analysis of the complex (Bundle et al., 1994b).

We report here an investigation of the bound conformation of a *Streptococcus* Group A trisaccharide hapten, propyl 3-*O*-(2-acetamido-2-deoxy-β-D-glucopyranosyl)-2-*O*-(α-L-rhamnopyranosyl)-α-L-rhamnopyranoside (**1**), bound by the anti-*Streptococcus* mouse monoclonal antibody, Strep 9. Immunological studies (Pinto et al., unpublished results) have shown that this trisaccharide, which displays the minimum repeating unit in the bacterial polysaccharide, is also the minimum unit which shows good inhibition of the antibody Strep 9. On the basis of these immunological studies, the binding constant for **1** was estimated to be on the order of 10^4 M^{-1}, which made it most likely that TRNOEs for the complex of **1** with Strep 9 would be observable. Various NOE and ROE experiments were performed to obtain information about the bound state of the ligand molecule. The SYBYL program (Tripos) was used for molecular mechanics and simulated annealing calculations to determine the conformation of bound **1**. Furthermore, with the aid of 1D and 2D NOE experiments, improved insights about the conformational preferences of the glycosidic linkages of the free trisaccharide in aqueous solution could be established.

MATERIALS AND METHODS

Trisaccharide **1** was synthesized according to a published protocol (Pinto et al., 1991). The monoclonal antibody Strep 9 (MW ~150 000) is a murine IgG3 antibody that was raised against pepsin-treated, heat-killed bacteria (Krause, 1970). It was purified from ascites fluid, first on immobilized protein A and then on a column of *N*-acetylglucosamine linked to agarose (Pinto et al., unpublished work).

Preparation of the NMR Samples. Trisaccharide **1** (15 mg, 27 mmol) was lyophilized from D_2O (99.9%, Isotec Inc.) five times and redissolved in 0.5 mL of D_2O (99.9%, Isotec Inc.). Five freeze−pump−thaw cycles were applied to remove dissolved oxygen before sealing under nitrogen, leading to a final concentration of 54 mM for **1**.

A solution of the intact antibody in PBS (phosphate-buffered saline; 10 mM KPO_4, 50 mM KCl, and 0.1 mM NaN_3, pH = 7.2) was transferred to a Centriprep concentrator (Amicon) with a cutoff range of 30 000 MW. The buffer was exchanged seven times with PBS−D_2O (pH = 7.2, not corrected for isotope effects), concentrated, and diluted to give a sample volume of 450 μL and then transferred to a 5-mm NMR tube. Determination of the absorbance at 280 nm (ϵ = 1.4 mg/mL) showed the presence of 40 nmol (6 mg) of antibody (80 nmol of binding sites) in this sample. A ligand stock solution was prepared so that it contained 80 nmol of **1** in 2 μL of D_2O (22.2 mg/mL). The antibody sample was titrated with this stock solution and the magnitude of the observed TRNOEs was monitored after each titration step with 1D transient NOE experiments. The final ligand:antibody ratio was 14:1 (2.2 mM **1**, 0.08 mM antibody).

NMR Experiments. All NMR experiments were carried out on a Bruker AMX 600 spectrometer operating at a ^1H frequency of 600.13 MHz with the sample nonspinning. All

2D experiments were acquired in phase-sensitive mode using time-proportional phase incrementation (Marion & Wüthrich, 1983). Data treatment was performed with standard UX-NMR (Bruker) software. Before integration, all spectra were baseline-corrected. Integration of 2D spectra was performed either by standard volume integration or by summation over the corresponding spectral rows and integration of the resulting projections with the one-dimensional integration routine. All NOESY and ROESY spectra were calculated with a $\pi/2$-shifted squared sine bell function in both dimensions.

NOE experiments of the free ligand **1** were performed at 316 and 284 K with a spectral width of 5.3 ppm. NOESY experiments were also performed at 316 and 284 K with a mixing time of 800 ms, 64 scans/ increment, 512 t_1 values, 2K data points in t_2, and a total relaxation delay of 4.3 s. The raw data were zero-filled to give a final data matrix of 1K × 2K ($F_1 \times F_2$). 1D Transient NOE experiments and data treatment were performed as described (Weimar et al., 1993; Peters & Weimar, 1994) with 80-ms Gaussian-shaped (Bauer et al., 1984) pulses (2K data points, truncation level 1%) for selective inversion. At 316 K, 1D transient NOE experiments were carried out on every resolved resonance with a corrected mixing time of 740 ms, 256 scans, 32 dummy scans, and a total relaxation delay of 4.3 s. 1D Transient NOE experiments at 284 K were performed on the resonance of H1A′ with the same parameters and corrected mixing times of 65, 105, 155, 205, 245, 305, 445, 645, and 1045 ms.

All NMR experiments of the antibody/trisaccharide complex were performed at 284 K. One set of 2D TRNOE spectra was recorded with a slightly modified NOESY pulse sequence using presaturation (1.5 s, 63 dB) and a 5-ms homospoil pulse in the middle of the mixing time (55, 105, 155, and 205 ms) to reduce the residual water signal. A spectral width of 12 ppm was recorded with 256 scans/ increment, resulting in an experimental time of ~70 h/2D TRNOE spectrum. The raw data matrices (512 × 2K, $t_1 \times t_2$) were zero-filled to give final matrices of 2K × 4K ($F_1 \times F_2$) data points.

A second set of 2D TRNOE spectra was acquired using a $T_{1\rho}$ filter (10 ms, 14 kHz) after the first $\pi/2$ pulse of the NOESY sequence (Scherf & Anglister, 1993) to reduce the protein background resonances. These experiments used presaturation (1.3 s, 62 dB) and a π pulse in the middle of the mixing time (50, 75, 95, 110, and 200 ms) followed by a 5-ms homospoil pulse to reduce the residual water signal. A spectral width of 5.7 ppm was recorded using 48 scans with data matrices of 384 × 2K ($t_1 \times t_2$) (total experimental time ~9 h/experiment) which were zero-filled to give a final matrix of 1K × 2K ($F_1 \times F_2$).

TRROESY experiments were acquired with the standard ROESY pulse sequence using the same spectral width as for the $T_{1\rho}$-filtered TRNOESY experiments, spin-lock fields of 100, 200, and 300 ms (5 kHz), 40 scans, and a raw data matrix of 320 × 2K ($t_1 \times t_2$) data points. Residual water was suppressed during the relaxation delay (1.3 s, 62 dB). Data treatment was performed as described for the $T_{1\rho}$-filtered TRNOESY experiments.

1D Transient NOE experiments of the antibody/ligand complex were performed as described for the free ligand (12 ppm spectral width) with presaturation during the relaxation delay (1.5 s, 63 dB) and a 5-ms homospoil pulse after the selective inversion pulse. For each 1D transient NOE spectrum, 2K scans preceded by 32 dummy scans were acquired.

After integration, distances for bound **1** were calculated with the isolated spin-pair approximation and extrapolated to zero mixing time according to the method of Baleja et al. (1990) with Excel (Microsoft).

Computations. All calculations were performed on a Silicon Graphics personal Iris 4D35 workstation. The standard force field within SYBYL 6.1 (Tripos) was used for grid-search, molecular mechanics, and simulated annealing calculations of systems in vacuo. All energy minimizations were performed with the Powell conjugate-gradient option (Powell, 1977). Grid search calculations of both glycosidic linkages in **1** were carried out with a 10° step size and a maximum number of 100 subsequent energy minimizations. While searching the angles at one glycosidic linkage, the other linkage was in the global minimum energy conformation. Constraints evaluated from TRNOESY or TRROESY spectra were used either as target distances or as a distance range to find the conformation of the bound ligand. The penalty function constant for the constraints was set to 100 kcal mol^{-1} $Å^{-2}$. Simulated annealing calculations started at 500 K at randomly chosen structures.

RESULTS AND DISCUSSION

NOE Experiments and Conformational Preferences of the Free Ligand 1. Initially, 1D and 2D NOE experiments for the free ligand **1** at 600 MHz were performed to permit a direct comparison with the TRNOE spectra to determine whether conformational changes were induced during the binding process. A temperature of 316 K was chosen for the NOE experiments of free **1** because at this temperature the HDO signal was placed between the resonances of the anomeric and the ring protons. In addition, due to the molecular tumbling, which is faster at 316 K compared to ambient temperature, the NOE effects are larger and therefore more readily observed. 1D Transient NOE experiments were also carried out at 284 K, the temperature at which the TRNOE spectra were recorded, to prove that the branched trisaccharide shows an NOE time dependence that one would expect for a molecule of this size in aqueous solution (Figure 1). The results of these experiments, performed on the resonance of H1A′, are shown in Figure 1a. The NOE effects are small and negative (maximum 1.4%). A NOESY experiment at 284 K also showed effects for the other long-range NOEs that were small and negative but of even lower magnitude than those for H1A′. At 316 K, both 1D transient NOE and NOESY experiments indicated that the NOE effects were of greater magnitude and positive.

Although some resonances of **1** showed small temperature-dependent shifts, the assignments of the proton resonances of **1** at 600 MHz did not differ from those reported previously at 400 MHz (Pinto et al., 1991; Kreis et al., 1995). So far, detailed conformational studies of **1** and other oligosaccharide fragments of the *Streptococcus* Group A polysaccharide have been carried out on the basis of ROESY data at 400 MHz in conjunction with molecular mechanics, molecular dynamics (Kreis et al., 1995), and Metropolis Monte Carlo calculations (Stuike-Prill & Pinto, 1995). Energy maps for the two glycosidic linkages of **1** computed with CHARMm (Brooks et al., 1983; Varma, 1993), PIMM91 (Smith &

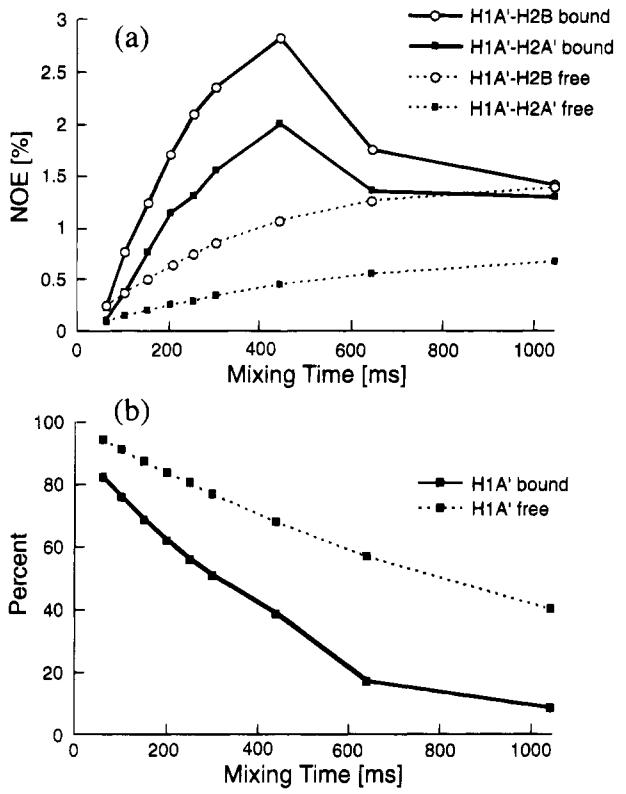

FIGURE 1: (a) Time dependence of the NOEs and TRNOEs H1A′−H2A′ and H1A′−H2B and (b) the decay of the selectively inverted signal H1A′ for free and bound **1**. Dotted and solid lines are for the free and bound species, respectively.

Lindner, 1991; Kroeker, 1993), GEGOP (Stuike-Prill & Meyer, 1991), and SYBYL (Tripos) are essentially equivalent, and therefore, further discussions will make use of the calculations performed with the SYBYL program to describe the conformational features of free and bound **1**.

It has been shown in the last few years that, due to steric hindrance around the branch point at the central unit, branched oligosaccharides such as **1** display a more rigid behavior in solution than their linear counterparts [see, for example, Bechtel et al. (1990), Yan and Bush (1990), Mukhopadhyay and Bush (1991), Miller et al. (1992), Kogelberg and Rutherford (1994), Rutherford et al. (1994), and Peters and Weimar (1994)]. Figure 2 shows the energy maps of the α-(1→2) and β-(1→3) linkages in **1**, calculated with the standard force field within SYBYL. One realizes that these maps only give an approximate view of the conformations of the two glycosidic linkages and the potential energy in this branched trisaccharide since computational restrictions required that the second linkage be kept in the global minimum conformation while optimizing the first. The global minimum conformation **I/III** of **1** (E_{rel} = 0.0 kcal/mol) is located around ϕ/ψ^2 = 59°/44° and ϕ/ψ = 58°/−50° for the α-(1→2) (**I**) and β-(1→3) (**III**) linkages, respectively. A second minimum **II** at the α-(1→2) linkage is found for the angles ϕ/ψ = 50°/−44° (E_{rel} = 1.9 kcal/mol) where only the ψ angle changes from its *+gauche* global minimum position to a *−gauche* position. In addition, the potential energy maps suggest a second local minimum energy conformation **IV** for the β-(1→3) linkage around ϕ/ψ = 170°/0°. Depending on the orientation of the α-(1→2) linkage, these conformations are up to ~5 kcal/mol higher in potential energy than the global minimum structure. This energy difference indicates that conformations in the area of minimum **IV** at the β-(1→3) linkage should not be populated to a high extent in aqueous solution. The ROESY spectra at 400 MHz of the previous conformational analysis showed no evidence for this second conformational family and nor did the molecular dynamics calculations (Kreis et al., 1995). The Metropolis Monte Carlo simulations (Stuike-Prill & Pinto, 1995), however, displayed some transitions between these two conformational states at the β-(1→3) linkage in **1**.

Figure 3 shows schematic representations of these two families of minimum energy conformations at the β-(1→3) linkage of trisaccharide **1**. Depending on the orientation of the α-(1→2) linkage and the rotational conformation of the *N*-acetyl methyl group in the area **IV** at the β-(1→3) linkage, a distance of ~2−3 Å between the *N*-acetyl methyl protons of the GlcNAc residue and H2A′ of the α-(1→2)-linked rhamnose residue occurs. This distance should give rise to a strong NOE enhancement if such conformations about the β-(1→3) linkage were populated to a significant extent in aqueous solution. In addition, this NOE is the only one which specifically accounts for conformations around **IV**

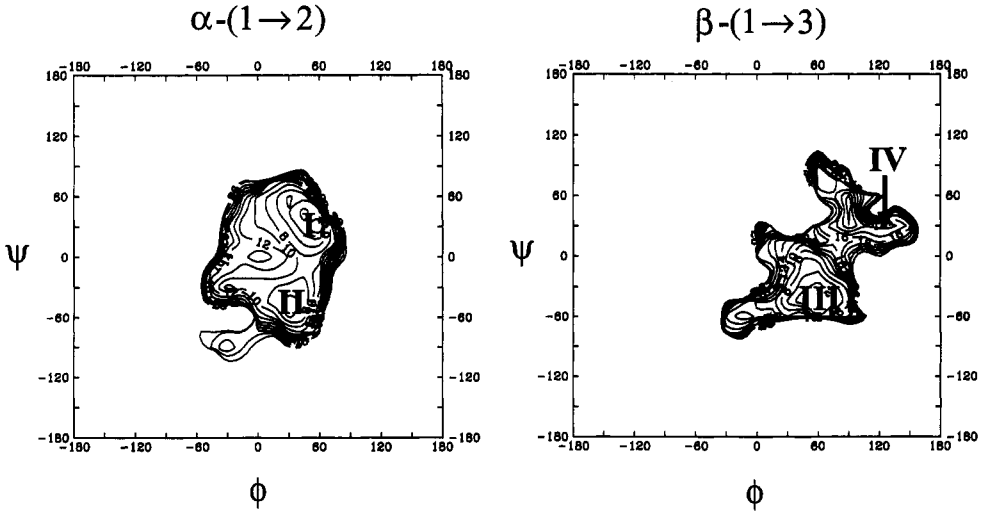

FIGURE 2: Energy maps of the α-(1→2) and β-(1→3) glycosidic linkages in **1**. The minimum energy conformations **I**, **II**, **III** and **IV** are indicated.

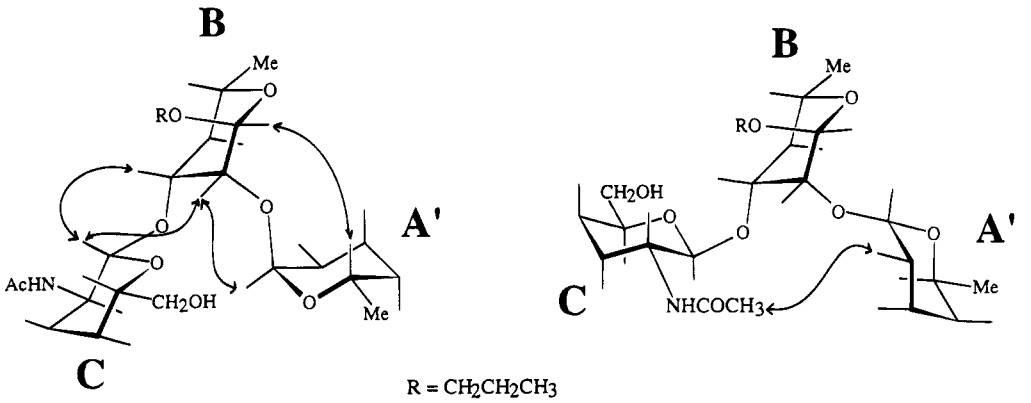

R = $CH_2CH_2CH_3$

FIGURE 3: Schematic representations of conformations from the areas **III** (left) and **IV** (right) at the β-(1→3) linkage of **1**. For minimum **III**, the major TRNOEs H1A′−H2B, H1B−H5A′, H1C−H3B, and H1C−H2B are indicated; for minimum **IV**, the NOE H*N*Ac−H2A′ is indicated. The hydroxyl groups are omitted for clarity.

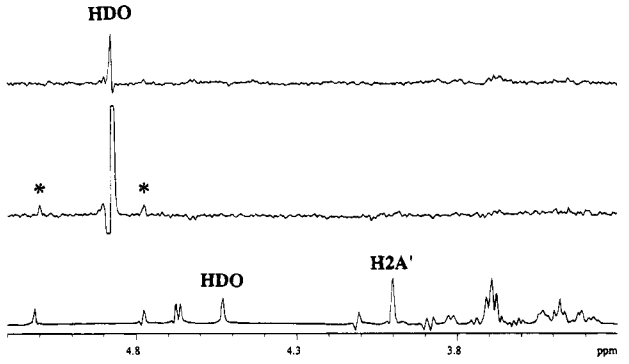

FIGURE 4: Comparison of 1D transient NOE spectrum (lower row, 840-ms mixing time) of uncomplexed **1** with cross sections at NCOMe from the TRNOESY (upper row, 200-ms mixing time) and ROESY (middle row, 200-ms spin-lock) spectra. The TRNOE cross sections were obtained from the $T1_\rho$-filtered TRNOESY spectrum. Peaks denoted with an asterisk result from T1 noise. Spectra were obtained at 284 K in PBS−D_2O; **1**:Ab = 14:1 (2.2 mM **1**, 0.08 mM Ab).

since it should be only observable in this area of conformational space. As can be seen from the NOE spectra in Figure 4 (1D transient of NAc), a very small NOE enhancement H*N*AcC-H2A′ could be observed in the NOE spectrum of free **1**. Therefore, this area of conformational space has to be populated by free **1** in aqueous solution. Since this NOE is very small, the percentage of conformations in this area has to be low, in agreement with their elevated potential energy.

The ROESY spectra for free **1** at 400 MHz showed five interglycosidic ROEs (H1A′−H2B, H1A′−H2C, H1B−H5A′, H1C−H2B, and H1C−H3B) (Kreis et al., 1995). All these five interactions could also be observed as strong but nevertheless small NOEs at 600 MHz (316 K). In addition, eight very small *long-range* NOEs (H1A′−H1B, H1A′−$H6_{pro\text{-}S}$C, H1A′−$H6_{pro\text{-}R}$C, H1A′−H4B, H1C−H4B, H2B−H4C+H5C, H2A′−H4B, and H*N*AcC−H2A′) (Figures 4−7 and data not shown) could be detected mainly with the aid of the 1D transient NOE experiment which shows better sensitivity of the NOE experiments performed at 600 MHz in comparison to the ROESY experiments at 400 MHz. As observed previously (Kreis et al., 1995), the interglycosidic NOEs H1A′−H2B and H1C−H3B are always larger than

[2] Dihedral angles at the glycosidic linkages are defined as ϕ (H1′−C1′−O1′−Cx), ψ (C1′−O1′−Cx−Hx), and ω (O6−C6−C5−O5), with x being the aglyconic site.

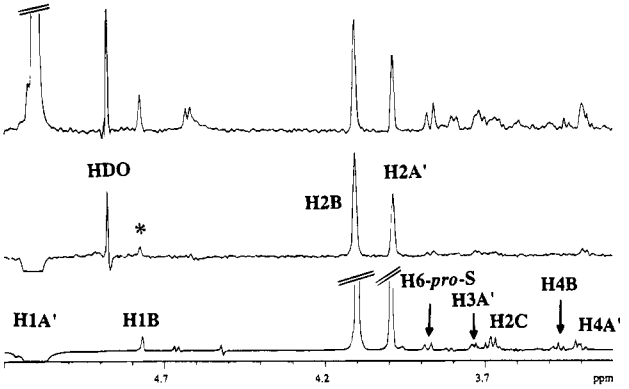

FIGURE 5: Comparison of 1D transient NOE spectrum (lower row, 840-ms mixing time) of uncomplexed **1** with cross sections at H1A′ from the TRNOESY (upper row, 200-ms mixing time) and ROESY (middle row, 200-ms spin-lock) spectra. Conditions were as described for Figure 4.

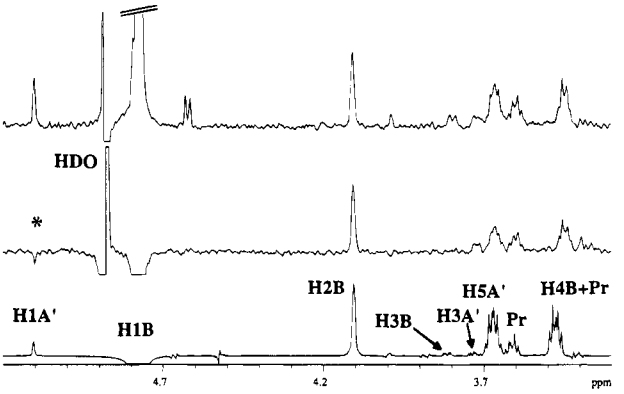

FIGURE 6: Comparison of 1D transient NOE spectrum (lower row, 840-ms mixing time) of uncomplexed **1** with cross sections at H1B from the TRNOESY (upper row, 200-ms mixing time) and ROESY (middle row, 200-ms spin-lock) spectra. Conditions were as described for Figure 4.

the intraglycosidic NOE H1A′−H2A′, indicating that the time-averaged distances corresponding to these interglycosidic NOEs are shorter than the distance H1A′−H2A′ (~2.5 Å) in the rhamnose ring.

Overlap of the $H6_{pro\text{-}R}$C and H3A′ signals does not permit an assessment of the conformational preference at the GlcNAc C5−C6 linkage in uncomplexed **1**. However, the vicinal $^3J_{H5,H6_{pro\text{-}SC}}$ coupling constant (1.2 Hz) is rather small and suggests a high percentage of *gg* conformations (Nishida et al., 1974; Haasnoot et al., 1980). In general, the whole

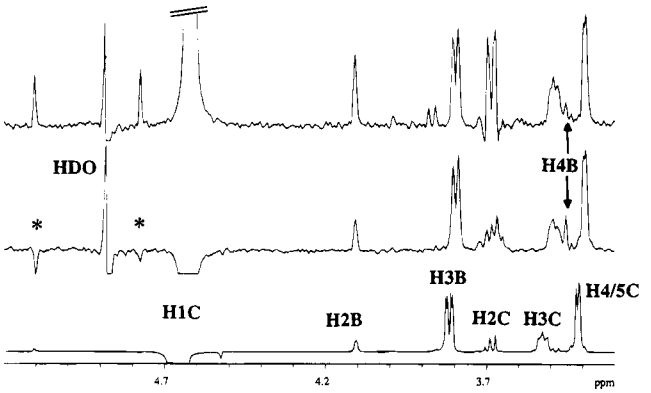

FIGURE 7: Comparison of 1D transient NOE spectrum (lower row, 840-ms mixing time) of uncomplexed **1** with cross sections at H1C from the TRNOESY (upper row, 200-ms mixing time) and ROESY (middle row, 200-ms spin-lock) spectra. Conditions were as described for Figure 4.

range of observed NOEs is not in agreement with a single conformation of uncomplexed **1**. On the contrary, these effects can only be interpreted with a model that samples all accessible conformations shown by the potential energy maps of the two glycosidic linkages, and therefore, we favor the model described by the Metropolis Monte Carlo simulations (Stuike-Prill & Pinto, 1995), which showed several transitions between the different conformations of trisaccharide **1**, over that described by molecular dynamics simulations (Kreis et al., 1995).

Optimizing Experimental Parameters To Measure TRNOEs. In order to determine the best experimental parameters for measuring TRNOEs, the solution of the antibody Strep 9 was titrated with a stock solution of the trisaccharide ligand at 284 K. The size of the observed NOEs was monitored with 1D transient NOE experiments by inverting the resonance of H1A′. Although the size of the observed negative NOEs was at a maximum at a ligand excess of 6:1, the titration showed no major change in magnitude until a ratio of 14:1 was reached. Here the NOEs started to decrease, and therefore, the titration was stopped. Increasing the temperature in several steps to 300 K did not change the magnitude of the observed NOEs significantly, so that an experimental temperature of 284 K was chosen in order to place the residual water resonance between the resonances of the anomeric protons of H1A′ and H1B, where it could be reduced without affecting the observed NOE effects. The sample showed no change in magnitude of the observed TRNOEs over several months when stored at 4 °C between the experiments.

TRNOEs or NOEs? The easiest way to distinguish between NOEs and TRNOEs in a ligand/receptor sample is usually by a change in sign (positive to negative) of the observed effects when comparing the free ligand NOEs with the corresponding TRNOEs. Here, however, the free ligand **1** shows negative NOEs at the temperature (284 K) at which the TRNOE experiments are performed. Therefore, it has to be proven that the observed NOEs for the trisaccharide/Strep 9 sample are indeed TRNOEs indicative of the conformation of the bound ligand and not just NOEs of the uncomplexed ligand. The time dependence of the NOE or TRNOE effects (NOE build up or NOE curve) is a better measure of whether the observed effects arise from a complexed ligand molecule because the bound ligand should show a different NOE time dependence than the free one. Thus, 1D transient NOE experiments were performed at 284 K with mixing times ranging from 65 to 1045 ms for free and bound **1**, inverting the resonances of H1A′ (Figure 1). From the magnitude of the NOE effects H1A′−H2B and H1A′−H2A′ and the decline of the inverted signal (selective T_1 relaxation times for H1A′ extracted from this decline: free **1**, 1150 ms; bound **1**, 320 ms), it is obvious that the NOEs in the antibody/ligand sample show a time dependence of a macromolecule, with a fast increase, a maximum of the NOE effect at around 400 ms mixing time, followed by a fast decrease (Neuhauss & Williamson, 1989). In comparison, free **1** does not reach this maximum NOE intensity at this temperature even at a mixing time of 1045 ms (Figure 1), which proves that the observed NOEs for the complex sample are in fact TRNOEs indicative of the bound state of the ligand. In addition, 1D transient NOE experiments with the sample of the complex were performed with total relaxation times of 4.5 and 1.2 s. These spectra were identical, indicating the fast T_1 relaxation for the complex. In a control NOE experiment, at 500 MHz, the antibody was substituted with BSA. At this field strength and at a temperature of 300 K, the observed NOEs were positive (data not shown), indicating that the observed TRNOEs for the sample of the antibody and the ligand **1** do not arise because of nonspecific binding or a viscous solution.

Determination of the Bound Conformation of Trisaccharide 1. The chemical shifts of bound and free **1** and the time-averaged resonances are identical when measured at the same temperature. The slight chemical-shift differences of some resonances (Figures 4−7) arise from the different temperatures between NMR experiments, 316 and 284 K for the free and bound ligand, respectively; these differences were corroborated by comparison of 1D spectra of the free ligand **1** acquired at 316 and 284 K. No significant increase in the line widths of the signals of bound **1** is observed, which shows that the ligand is in fast exchange on the chemical-shift time scale.

Examination of Figure 1 indicates that even the strong TRNOEs for bound **1** are just in the range of a few percent at optimum mixing time. Together with the relatively low concentration of **1** (~2.2 mM), a large number of experiments with the standard NOESY pulse sequence had to be performed to obtain a good signal-to-noise ratio, resulting in an experimental time of ~70 h for each of these TRNOE spectra. A second set of TRNOE spectra made use of a $T_{1\rho}$ filter after the first $\pi/2$ pulse in the NOESY pulse sequence (Scherf & Anglister, 1993). This resulted in complete relaxation of the antibody resonances, and therefore, the receiver gain setting on the spectrometer could be changed from 1K for the normal NOESY experiment to 8K for the $T_{1\rho}$ filter sequence since no protein signals had to be recorded. The time required for these experiments could thus be reduced to ~9 h with additional improvement in the quality of the spectra. In addition, 1D transient NOE experiments with different mixing times were performed by inverting the resonances of H1A′, H1B, H1C, H2A′, and H2B to investigate which experiment would give the most accurate distance constraints when the small TRNOEs arising from these signals were integrated.

The absolute magnitude of the observed TRNOEs made it impossible to acquire spectra with a mixing time shorter than 50 ms to prevent spin diffusion; at 50 ms the effects were hardly visible. At longer mixing times, however, all

interglycosidic NOEs of the free ligand **1** could be observed as TRNOEs (compare Figures 4−7). A first attempt to extract interproton distances from the TRNOE spectra (see below) led to values between 2.8 and 3.2 Å for the *long-range* TRNOEs. These distances are much too short to fit an appropriate model of bound **1**. Campbell and Sykes (1991) have shown that spin diffusion can give rise to virtual distances as short as 2.5 Å in TRNOE spectra. We concluded, therefore, that spin diffusion could play a major role especially for the *long-range* TRNOEs in the bound carbohydrate ligand. To determine the amount of spin diffusion in the observed TRNOE effects, a set of TRROESY spectra with different spin-lock mixing times was acquired. Cross peaks arising exclusively from spin diffusion would have the same sign as the diagonal signals, making them easy to differentiate from first-order TRROE effects, which would have the opposite sign (Neuhauss & Williamson, 1989b). A lack of cross peaks in the ROESY spectra would be due either to a lack of magnetization transfer or to a cancellation of TRROE transfer by the spin diffusion effect.

Figures 4−7 show examples of cross sections from TRNOE and TRROE spectra of bound **1** in comparison to 1D transient NOE spectra of free **1**. The TRNOE and TRROE cross sections are scaled so that the major effect has the same size in both spectra. Therefore, it is apparent which of the smaller effects is affected by spin diffusion. Not surprisingly, all the *long-range* TRNOEs show a strongly reduced intensity or are not observable at all in the TR-ROESY spectra. Only the interglycosidic TRNOEs H1A′−H2B and H1C−H3B seemed not to be influenced by spin diffusion. The TRNOEs H1C−H2B and H1B−H5A′ show some reduction in magnitude in the ROESY spectra, implying that some spin diffusion exists. A complication in interpreting the ROESY spectra arises from the appearance of some secondary HOHAHA effects (Bax, 1988; Neuhauss & Keeler, 1986) (compare the enhancement of H4B in Figure 7). These effects are the only ones which are actually larger in the ROESY spectra than in the TRNOE spectra and thus can be distinguished from primary cross-relaxation effects.

The only dipolar contact of free **1** which could not be observed as a TRNOE or TRROE effect in either the 1D or 2D spectra of the antibody/trisaccharide complex is the NOE HNAc−H2A′ (see Figure 4). Therefore, conformations in the area **IV** of the β-(1→3) linkage (Figure 2) are not bound by the antibody Strep 9.

No crystal structure of the antibody Strep 9 is available and only a range for the off rate of the complex can be estimated from inhibition data. A rigorous treatment of the observed TRNOEs based on the complete relaxation matrix approach (Ni & Zhu, 1994; Ni & Scheraga, 1994; Lian et al., 1994) is, therefore, not readily achieved. Although there are new methods for determining off rates (Davis et al., 1994) and that account for spin diffusion which do not rely on a knowledge of protein structure (Lai et al., 1993; Constantine et al., 1995), in our case, a quantitation of the TRNOEs was made with the isolated two-spin approximation and the method of Baleja et al. (1990). Figure 8 and Table 1 show the extrapolation of distances to zero mixing time for the three major interglycosidic (H1A′−H2B, H1B−H5A′, and H1C−H3B) and one intraglycosidic (H1C−H3C) TRNOEs. Distances extracted from relative integrals of the 1D transient NOE spectra yielded the smallest variations of the experimental data points. The two sets of 2D TRNOE data gave essentially the same information but with larger experimental errors (data not shown). Comparison of the distances extrapolated from the integrals of the TRROESY spectra with those determined from the TRNOESY spectra yielded differences of less than ±0.1 Å (see Table 1). The spin diffusion contribution to the NOE H1C−H2B is quite high, so that we only used the integrals from the TRROESY spectra to extrapolate the corresponding distance that was used in the calculations but with a higher uncertainty (see Table 1). An estimate of the accuracy of the distances thus obtained can be made by comparing the experimental value derived from the intraglycosidic TRNOE H1C−H3C with the actual distance between these two protons in the carbohydrate ring system (Table 1). The experimental value (2.6 Å) is practically identical to the distance measured from the relaxed molecular model, so it is likely that the other experimentally derived distances are also accurate. Overall, the experimental error in the distance constraints should be smaller than ±0.1 Å.

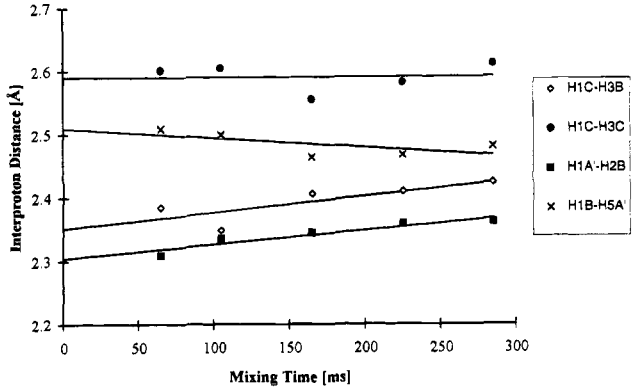

FIGURE 8: Extrapolation of distances, calculated with the isolated two-spin approximation, to zero mixing time. The experimental TRNOE data points are indicated.

Table 1: Compilation of Distances Extracted from TRNOE and TRROE Experiments Used for Simulated Annealing Calculations in Comparison to the Corresponding Values for Bound **1** after Calculations[a]

dipolar interaction	distances extracted from TRNOE spectra	distances extracted from TRROE spectra	distance constraints (range) used for simulated annealing and minimization calculations	distances for bound **1** after calculations
H1A′−H2B	2.30	2.25	2.30 (±0.05)	2.33
H1B−H5A′	2.51	2.60	2.55 (±0.10)	2.58
H1C−H3B	2.35	2.35	2.35 (±0.05)	2.36
H1C−H2B	nd[b]	3.30	3.20 (±0.15)	3.27
H1C−H3C	2.61	2.74		2.60
H1A′−H2C			<3.75	4.90
H1A′−H6$_{proR}$C			<3.65	3.70

[a] All distances are given in angstroms. [b] nd, not determined because of the influence of spin diffusion.

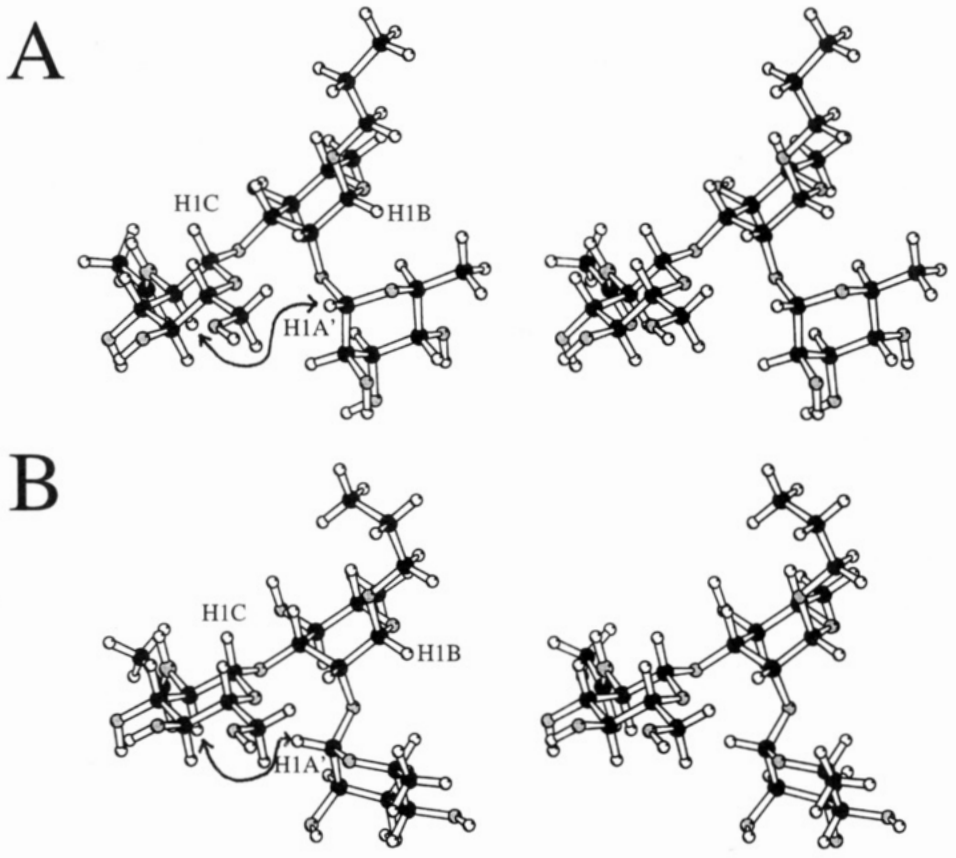

FIGURE 9: Stereo representations of (A) the antibody-bound and (B) the global minimum conformations of **1**, drawn with molscript (Kraulis, 1991). Double-headed arrows indicate the H1A′−H2C distance [4.65 Å in (A) and 2.75 Å in (B)].

Of equal importance as the distance constraints in defining the bound conformation of a ligand molecule are the repulsive constraints derived from the absence of NOEs, as shown in the following. Using the TRNOE- (TRROE-) derived distance constraints within the minimization option of SYBYL, a conformation which satisfied all these constraints could easily be derived. This conformation, which is very close to the global minimum conformation of **1**, shows glycosidic torsion angles ϕ/ψ = 45°/26° and 54°/−46° (E_{rel} = 4.8 kcal/mol) for the α-(1→2) and β-(1→3) linkages, respectively. However, in this conformation, the protons H2C and H1A′ are at a distance of ∼3 Å which should give rise to an observable TRNOE. It should be noted that the intraglycosidic distance H1C−H2C is in the same range and the corresponding NOE effect is readily detectable (see Figure 7; TRNOEs of H1C). Figure 5 shows that the enhancement H1A′−H2C in the TRNOE spectrum is due to spin diffusion since no signal can be detected in the TRROESY spectrum.

We recognize that the observed TRNOE effects are weak and that the NOE H1A′−H2C may be further attenuated by residual dynamics in the bound state (Abseher et al., 1995) or by protein-mediated magnetization leakage. However, the absence of the H1A′−H2C contact, within the experimental error, certainly suggests that the bound ligand exists in minimum **II** and not in minimum **I** about the α-L-(1→2) linkage. To incorporate this additional information in the calculation, an upper distance limit for the observation of TRNOEs had to be defined. Usually intraglycosidic TRNOEs can be used as a gauge for this purpose since they arise from magnetization transfer in the carbohydrate ring system and are therefore not subject to possible distance fluctuations. As mentioned above, the secondary HOHAHA effects (Bax, 1988; Neuhauss & Keeler, 1986) made it somewhat difficult to define the upper limit since they gave rise to some unusual strong intraglycosidic TRROE enhancements. A distance of 3.75 Å was judged to be at the limit to permit observation of a very small enhancement and was therefore incorporated into the constraints table as a minimum distance for a non-TRROE effect between H1A′ and H2C. With this additional constraint, several simulated annealing calculations were performed starting from randomly chosen conformations and a starting temperature of 500 K. Higher starting temperatures resulted in twisted and inverted ring systems and are therefore not suitable.

The calculations now yielded two different conformations for **1** which satisfied the distance constraints. One was close to the global minimum conformation **I** and the second one was close to minimum **II** at the α-(1→2) linkage. Both conformations showed the β-(1→3) linkage in conformation **III** and displayed a high potential energy. The constraint between H1A′ and H2C in these two models was deleted and the conformers were again minimized. They converged on the minimum energy conformations **I** and **II** at the α-(1→2) linkage, with the β-(1→3) linkage still in conformation **III**. The conformer which showed the α-(1→2) linkage in minimum **II** now yielded a distance between H1A′ and H2C of ∼4.9 Å, which is much too large to observe a TRNOE(ROE) effect, consistent with the experimental data. Therefore, the bound conformation of **1** has to be close to minima **II** and **III** at the two glycosidic linkages. A distance of approximately 3 Å between the protons H1A′ and $H6_{pro\text{-}S(R)}C$ in this conformation indicated the need for additional repulsive constraints since the corresponding effects in the

TRROE spectra are extremely weak (see Figure 5). Definition of the target distances for these two effects as 3.65 Å now required only very small conformational changes in both glycosidic linkages to satisfy all of the TRNOE(ROE) and non-TRNOE(ROE) constraints. The resulting conformation has the glycosidic angles ϕ/ψ = 50°/−44° and 56°/−46° (E_{rel} = 2.3 kcal/mol) for the α-(1→2) and β-(1→3) linkages, respectively, and is shown in Figure 9, together with the global minimum conformation **I/III** (see also Table 1).

A model of the *Streptococcus* Group A cell-wall polysaccharide has been constructed from averaged angles of minimum energy conformations of several oligosaccharide portions of this polymer (Kreis et al., 1995) with angles for the α-(1→2) and β-(1→3) glycosidic linkages that are very close to those obtained here for the global minimum conformation **I/III**. The only substantial difference between this model of the polysaccharide and the bound conformation of the ligand molecule **1** established in this work is that the ψ angle at the α-(1→2) linkage is changed from a *+gauche* to a *−gauche* orientation (Figure 9). At least with respect to this glycosidic linkage, the antibody Strep 9 selects a conformation of the hapten **1** which is not the global minimum. This analysis has implications for the conformation of the cell-wall polysaccharide in the uncomplexed vs the complexed state. If the observed global minimum conformation **I/III** of trisaccharide **1** and other oligomer portions of the polymer (Kreis et al., 1995; Stuike-Prill & Pinto, 1995) is also representative of this unit in the intact *Streptococcus* Group A polysaccharide, then complexation of the polysaccharide by antibody induces a conformational change, at least at the α-(1→2) linkage.

CONCLUSIONS

Although the ligand **1** is a branched trisaccharide, this study shows that it is not a rigid molecule when free in solution. Improved NOE data are only in accord with a molecule adopting a range of conformations at both glycosidic linkages of **1**. Of particular note, the NOE H*N*Ac−H2A′ accounts for a conformation at the β-(1→3) linkage with a ϕ angle rotated to ~180°. This conformation has been predicted previously by Metropolis Monte Carlo (Stuike-Prill & Pinto, 1995) but not by molecular dynamics simulations (Kreis et al., 1995), suggesting that Metropolis Monte Carlo simulations may be better able to represent the conformational space occupied by this branched trisaccharide.

TRNOE and TRROE experiments for the complex of this trisaccharide with the monoclonal antibody Strep 9 showed very small TRNOE effects together with spin diffusion effects that complicated the extraction of interglycosidic distances for complexed **1**. TRROE experiments on the complex were absolutely necessary to solve the complexed conformation of the ligand in that the spin diffusion contribution to the observed TRNOE effects could be addressed. Distances extracted from the experiments were in accord with two conformations of the ligand, but only one of them satisfied additional repulsive constraints, derived from the absence of TRROE effects. This analysis demonstrates that the explicit inclusion of such repulsive constraints in the calculations can be as equally important as TRNOE-derived distances in the conformational analysis of a bound ligand molecule. The complexation of trisaccharide **1** by the complementary antibody Strep 9 results in the selection of a conformation which is very close to a local minimum energy conformation for the uncomplexed ligand.

ACKNOWLEDGMENT

We are grateful to U. C. Kreis for performing the PIMM calculations and for helpful discussions.

REFERENCES

Abseher, R., Lüdemann, S., Schreiber, H., & Steinhauser, O. (1995) *J. Mol. Biol. 249*, 604−624.
Albrand, J. P., Birdsall, B., Feeney, J., Roberts, G. C. K., & Burgen, A. S. V. (1979) *Int. J. Biol. Macromol. 1*, 37−41.
Arepalli, S. R., Glaudemans, C. P. J., Daves, G. D., Jr., Kovác, P., & Bax, A. (1995) *J. Magn. Reson. B 106*, 195−198.
Asensio, J. L., Caqada, J., & Jimenez-Barbero, J. (1995) *Eur. J. Biochem.* (in press).
Balaram, P., Bothner-By, A. A., & Breslow, E. (1972b) *J. Am. Chem. Soc. 94*, 4017−4018.
Balaram, P., Bothner-By, A. A., & Dadok, J. (1972a) *J. Am. Chem. Soc. 94*, 4015−4017.
Baleja, J. D., Moult, J., & Sykes, B. D. (1990) *J. Magn. Reson. 87*, 375−384.
Bauer, C., Freeman, R., Frenkiel, T., Keeler, J., & Shaka, A. J. (1984) *J. Magn. Reson. 58*, 442−457.
Bax, A. (1988) *J. Magn. Reson. 77*, 134−147.
Bax, A., & Davis, D. G. (1985) *J. Magn. Reson. 63*, 207−213.
Bechtel, B., Wand, A. J., Wrobleswski, K., Koprowski, H., & Thurin, J. (1990) *J. Biol. Chem. 265*, 2028−2037.
Bisno, A. L. (1985) in *Nonsuppurative Poststreptococcal Sequelae: Rheumatic Fever and Glomerulonephritis in Principles and Practice of Infectious Diseases*, 2nd Ed. (Mandell, G. L., Douglas, R. G., & Bennett, J. E., Eds.) Chapter 160, p 1133, Wiley, New York.
Boelens, R., Koning, T. M. G., van der Marel, G. A., van Boom, J. H., & Kaptein, R. J. (1989) *J. Magn. Reson. 82*, 290−308.
Borgias, B. A., & James, T. L. (1989) *Methods Enzymol. 176*, 169−183.
Bothner-By, A. A., Stephens, R. L., Lee, J., Warren, C. D., & Jeanloz, R. W. (1984) *J. Am. Chem. Soc. 106*, 811−813.
Brooks, B. R., Bruccoleri, R. E., Olafson, B. D., States, D. J., Swaminathan, S., & Karplus, M. (1983) *J. Comput. Chem. 4*, 187−217.
Bundle, D. R., Eichler, E., Gidney, M. A. J., Meldal, M., Ragauskas, A., Sigurskjold, B. W., Sinnott, B., Watson, D. C., Yaguchi, M., & Young, N. M. (1994a) *Biochemistry 33*, 5172−5182.
Bundle, D. R., Baumann, H., Brisson, J.-R., Gagné, S. M., Zdanov, A., & Cygler, M. (1994b) *Biochemistry 33*, 5183−5192.
Cagas, P., & Bush, C. A. (1992) *Biochemistry 32*, 277−292.
Campbell, A. P., & Sykes, B. D. (1991) *J. Magn. Reson. 93*, 77−92.
Campbell, A. P., & Sykes, B. D. (1993) *Annu. Rev. Biophys. Biomol. Struct. 22*, 99−122.
Clore, G. M., & Gronenborn, A. M. (1982) *J. Magn. Reson. 48*, 402−417.
Clore, G. M., & Gronenborn, A. M. (1983) *J. Magn. Reson. 53*, 423−442.
Coligan, J. E., Kindt, T. J., & Krause, R. M. (1987) *Immunochemistry 15*, 755−760.
Constantine, K. L., Friedrichs, M. S., Detlefsen, D., Nishio, M., Tsunakawa, M., Furumai, T., Ohkuma, H., Oki, T., Hill, S., Bruccoleri, R. E., Lin, P.-F., & Mueller, L. (1995) *J. Biomol. NMR 5*, 271−286.
Cygler, M., Rose, D. R., & Bundle, D. R. (1991) *Science 253*, 442−445.
Davis, D. G., Perlman, M. E., & London, R. E. (1994) *J. Magn. Reson. B104*, 266−275.
Fischetti, V. A. (1989) *Clin. Microbiol. Rev. 2*, 285−314.
Glaudemans, C. P. J., Lerner, L., Daves, G. D., Jr., Kovác, P., Venable, R., & Bax, A. (1990) *Biochemistry 29*, 10906−10911.
Goldstein, I. J., Halpern, B., & Roberts, L. (1967) *Nature 213*, 44−47.
Goldstein, I. J., Rebeyrotte, P., Parlebas, J., & Halpern, B. (1968) *Nature 219*, 866−868.

Haasnoot, C. A. G., de Leeuw, F. A. A. M., & Altona, C. (1980) *Tetrahedron 36*, 2783−2792.
Huang, D. H., Krishna, N. R., & Pritchard, D. G. (1986) *Carbohydr. Res. 155*, 193−199.
Kogelberg, H., & Rutherford, T. J. (1994) *Glycobiology 4*, 49−57.
Kraulis, P. J. (1991) *J. Appl. Crystallogr. 24*, 946−950.
Krause, R. M. (1970) *Adv. Immunol. 12*, 1−56.
Kreis, U. C., Varma, V., & Pinto, B. M. (1995) *Int. J. Biol. Macromol. 17*, 117−130.
Kroeker, M. (1993) Ph.D. Thesis, Technical University Darmstadt, Germany.
Lai, X., Chen, C., & Andersen, N. H. (1992) *J. Magn. Reson. B101*, 271−288.
Lian, L. Y., Baruskov, I. L., Sutcliffe, M. J., Sze, K. H., & Roberts, G. C. K. (1994) *Methods Enzymol. 239*, 657ff.
Marino-Albernas, J.-R., Harris, S. L., Varma, V., & Pinto, B. M. (1993) *Carbohydr. Res. 245*, 245−257.
Marion, D., & Wüthrich, K. (1983) *Biochem. Biophys. Res. Commun. 113*, 967−974.
Miller, K. E., Mukhopadhyay, C., Cagas, P., & Bush, C. A. (1992) *Biochemistry 31*, 6703−6709.
Mukhopadhyay, C., & Bush, C. A. (1991) *Biopolymers 31*, 1737−1746.
Neuhauss, D., & Keeler, J. (1986) *J. Magn. Reson. 68*, 568−574.
Neuhauss, D., & Williamson, M. P. (1989a) *The Nuclear Overhauser Effect in Structural and Conformational Analysis*, pp 133−134, VCH Publishers, Inc., New York.
Neuhauss, D., & Williamson, M. P. (1989b) *The Nuclear Overhauser Effect in Structural and Conformational Analysis*, p 312, VCH Publishers, Inc., New York.
Ni, F., & Scheraga, H. A. (1994) *Acc. Chem. Res. 27*, 257−264.
Ni, F., & Zhu, Y. (1994) *J. Magn. Reson. B 102*, 180−184.
Nishida, Y., Ohrui, H., & Meguro, H. (1974) *Tetrahedron Lett.* 1575−1578.
Perlman, M. E., Davis, D. G., Koszalka, G. W., Tuttle, J. V., & London, R. E. (1994) *Biochemistry 33*, 7547−7559.
Peters, T., & Weimar, T. (1994) *J. Biomol. NMR 4*, 97−116.
Pinto, B. M. (1993) *ACS Symp. Ser. 519*, 111−131.
Pinto, B. M., Reimer, K. B., & Tixidre, A. (1991) *Carbohydr. Res. 210*, 199−219.
Poppe, L., Stuike-Prill, R., Meyer, B., & van Haalbeek, H. (1992) *J. Biomol. NMR 2*, 109−136.
Powel, M. J. D. (1977) *Math. Program. 12*, 241−254.
Read, S. E., & Zabriskie, J. B., Eds. (1980) *Streptococcal Diseases and the Immune Response*, Academic Press, New York.
Rotta, J. (1987) in *Towards Better Carbohydrate Vaccines* (Bell, R., & Torrigiani, G., Eds.) John Wiley & Sons, New York, pp 203−218.
Rutherford, T. J., Spackman, D. G., Simpson, P. J., & Homans, S. W. (1994) *Glycobiology 4*, 59−68.
Scherf, T., & Anglister, J. (1993) *Biophys. J. 64*, 754−761.
Sigurskjold, B. W., Altman, E., & Bundle, D. R. (1991) *Eur. J. Biochem. 197*, 239−246.
Sigurskjold, B. W., & Bundle, D. R. (1992) *J. Biol. Chem. 267*, 8371−8376.
Smith, A. E., & Lindner, H. J. (1991) *J. Comput. Aided Mol. Des. 2*, 235−262.
Stuike-Prill, R., & Meyer, B. (1991) *Eur. J. Biochem. 194*, 903−919.
Stuike-Prill, R., & Pinto, B. M. (1995) *Carbohydr. Res.* (in press).
Varma, V. (1993) Ph.D. Thesis, Simon Fraser University, Burnaby, B. C., Canada.
Weimar, T., Meyer, B., & Peters, T. (1993) *J. Biomol. NMR 3*, 399−414.
Williams, R. C. (1993) in *Clinical Aspects of Immunology*, 5th Ed. (Lachmann, P. J. L., Peters, K., Rosen, F. S., & Wright, M. J., Eds.) Vol. 3, pp 1671−1683, Blackwell Scientific Publishers, Boston, MA.
Yan, Z. Y., & Bush, C. A. (1990) *Biopolymers 29*, 799−812.

BI951367X